doi:10.1093/brain/awz170 BRAIN 2019: 142; 2336–2351 | 2336

BRAIN
A JOURNAL OF NEUROLOGY

Parallel pathways of seizure generalization

Natalia Dabrowska,[1,*] Suchitra Joshi,[1,*] John Williamson,[1] Ewa Lewczuk,[1] Yanhong Lu,[2] Samrath Oberoi,[3] Anastasia Brodovskaya[4] and Jaideep Kapur[1,5,6]

*These authors contributed equally to this work.

Generalized convulsive status epilepticus is a life-threatening emergency, because recurrent convulsions can cause death or injury. A common form of generalized convulsive status epilepticus is of focal onset. The neuronal circuits activated during seizure spread from the hippocampus, a frequent site of seizure origin, to the bilateral motor cortex, which mediates convulsive seizures, have not been delineated. Status epilepticus was initiated by electrical stimulation of the hippocampus. Neurons transiently activated during seizures were labelled with tdTomato and then imaged following brain slice clearing. Hippocampus was active throughout the episode of status epilepticus. Neuronal activation was observed in hippocampus parahippocampal structures: subiculum, entorhinal cortex and perirhinal cortex, septum, and olfactory system in the initial phase status epilepticus. The tdTomato-labelled neurons occupied larger volumes of the brain as seizures progressed and at the peak of status epilepticus, motor and somatosensory cortex, retrosplenial cortex, and insular cortex also contained tdTomato-labelled neurons. In addition, motor thalamic nuclei such as anterior and ventromedial, midline, reticular, and posterior thalamic nuclei were also activated. Furthermore, circuits proposed to be crucial for systems consolidation of memory: entorhinal cortex, retrosplenial cortex, cingulate gyrus, midline thalamic nuclei and prefrontal cortex were intensely active during periods of generalized tonic-clonic seizures. As the episode of status epilepticus waned, smaller volume of brain was activated. These studies suggested that seizure spread could have occurred via canonical thalamocortical pathway and many cortical structures involved in memory consolidation. These studies may help explain retrograde amnesia following seizures.

1 Department of Neurology, University of Virginia, Charlottesville, VA 22908, USA
2 College of Arts and Sciences, University of Virginia, Charlottesville, VA 22908, USA
3 Department of Biomedical Engineering, University of Virginia, Charlottesville, VA 22908, USA
4 Neuroscience Graduate Program, University of Virginia, Charlottesville, VA 22908, USA
5 UVA Brain Institute, University of Virginia, Charlottesville, VA 22908, USA
6 Department of Neuroscience, University of Virginia, Charlottesville, VA 22908, USA

Correspondence to: Jaideep Kapur MD, PhD
UVA Brain Institute, University of Virginia, Health Sciences Center, PO Box: 801330,
Charlottesville, VA 22908, USA
E-mail: jk8t@virginia.edu

Keywords: status epilepticus; neuronal activation maps; TRAP; passive tissue clearing; unbiased whole-brain imaging

Abbreviations: DGC = dentate granule cell; TRAP = targeted recombination in active populations

Introduction

Seizures result from abnormal, excessive or a synchronous increase in neuronal activity, which can spread across brain regions activating local and large-scale circuits, leading to behavioural manifestations. Hughlings Jackson first recognized that convulsive movements of the face, arms and legs occur when seizures spread to the motor cortex (York and

Received September 17, 2018. Revised April 18, 2019. Accepted April 23, 2019. Advance Access publication June 25, 2019

Steinberg, 2011). It is currently proposed that focal seizures spread to subcortical centres via projections to the thalamus and widespread thalamocortical interconnections then cause rapid activation of both hemispheres causing secondarily generalized tonic-clonic seizures (Westbrook, 2000, 2015). In several previous studies that used radiolabelled 2-deoxyglucose (2-DG) and cFos staining, motor cortical fields in the prefrontal and frontal cortex did not display increased radiolabelled 2-DG uptake or cFos immunoreactivity during the prolonged seizures observed in status epilepticus (Van Landingham and Lothman, 1991; White and Price, 1993). In other studies, variable activation of the motor cortex was reported (Handforth and Ackermann, 1988; Handforth and Treiman, 1995). Whether motor cortex is activated during seizure generalization in humans is also unclear; reduced cerebral blood flow in frontoparietal association cortex is observed in patients during pre-generalization and generalization periods of focal seizures (Blumenfeld *et al.*, 2003, 2009*a*).

Expression of immediate early genes such as cFos and Arc increase transiently in active neurons following calcium influx through glutamate receptors and voltage-gated calcium channels (Sheng and Greenberg, 1990). The expression of cFos has been used extensively to construct neuronal activity maps because the technique provides cell-level spatial resolution. However, Fos protein is upregulated transiently, has poor temporal resolution, and there is a low signal-to-noise ratio (Morgan *et al.*, 1987; Le Gal La Salle, 1988; Guenthner *et al.*, 2013). Several immediate early gene promoter-controlled fluorescent protein-based methods have been developed to tag active neurons in transgenic or knock-in mice (Barth *et al.*, 2004; Kawashima *et al.*, 2014) and have been used to study brain functions such as the memory trace (Garner *et al.*, 2012). These methods combine the sensitivity of immediate early gene expression with the permanence of fluorescent protein expression and their high signal-to-noise ratio.

We used TRAP (targeted recombination in active populations) mice, which adds temporal resolution to cFos tagging to visualize neurons activated by seizures (Guenthner *et al.*, 2013). Seizures were initiated in the hippocampus using an electrical stimulation method recently adapted for mice (Lothman *et al.*, 1989; Lewczuk *et al.*, 2018). In this model of status epilepticus, seizure evolved over a period of hours, increasing in intensity, reaching a peak where multiple generalized tonic-clonic seizures occurred and then became less intense before ending. Tissue clarification (Yang *et al.*, 2014) and confocal imaging/processing allowed visualization of TRAPed neurons with minimal disruption of neuronal networks.

Materials and methods

Animals

All animals were handled according to a protocol approved by the University of Virginia Animal Care and Use Committee. Mice expressing Cre-ER under the regulation of the cFos promoter (B6.129(Cg)-*Fos*$^{tm1.1(cre/ERT2)Luo}$/J, Jackson Laboratories, Bar Harbor, ME, #021882) and mice expressing tdTomato from the Rosa locus (B6.Cg-*Gt(ROSA)26Sor*$^{tm9(CAG-tdTomato)Hze}$/J, Jackson Laboratories, Bar Harbor, ME, #007909) were bred to generate TRAP mice (Guenthner *et al.*, 2013). The genotyping was performed using a kit from KAPA Biosystems. Four animals per cage were maintained in a 12 h light/12 h dark cycle and had *ad libitum* access to food and water. Adult (22–25 g) mice of both sexes were used in the experiments. All common chemicals were purchased from Sigma-Aldrich and the photoactivator compound VA044 was obtained from Wako Chemicals.

Induction of status epilepticus and EEG recording

Implantation of left ventral hippocampal and bilateral cortical electrodes and induction of status epilepticus using continuous hippocampal stimulation was carried out as described previously (Lewczuk *et al.*, 2018). At the end of the stimulation period, animals exhibiting self-sustained seizure activity with high frequency (>1 Hz) rhythmic spikes were considered to be in status epilepticus (Supplementary Fig. 1B). The end of status epilepticus was marked by arrhythmic spiking, <1 Hz frequency. Cohorts of animals were treated with 4-hydroxy tamoxifen (4-OHT, 50 mg/kg) at 60, 120, 180, 240 and 300 min from the start of hippocampal stimulation; each animal received a single injection of 4-OHT. To allow maximal expression of tdTomato in TRAPed neurons, the animals were perfused 7 days after 4-OHT injection.

Passive clarity technique

A tissue clearing protocol described in a previous study was used (Yang *et al.*, 2014). Briefly, animals were transcardially perfused with a solution of 0.1 M phosphate-buffered saline (PBS) pH 7.4 containing 4% paraformaldehyde and 4% acrylamide. The brains were incubated overnight at 4°C in the same solution and then 200-µm thick sections of the entire brain were prepared on a vibratome (Leica 3200). The sections were incubated in 1% acrylamide in PBS containing the photoactivator compound, 0.25% VA044, overnight in the dark at 4°C. The tissue was degassed and polymerized at 37°C for 2 h, followed by washes with PBS to remove unpolymerized and excess acrylamide. The sections were incubated in PBS containing 8% SDS at 37°C until they became transparent, usually for 24 to 36 h, then washed three times with PBS containing 0.1% Triton^{TM} X-100 (PBST) for 30 min each, and processed for immunolabelling (Supplementary Fig. 1C).

Immunohistochemistry

Immunohistochemistry was carried out as described previously (Sun *et al.*, 2007). The antibodies used were anti-cFos antibody (1:300, sc52, Santa Cruz Biotechnology), anti-NeuN antibody (1:200, MAB377, Millipore), anti-GFAP antibody (1:300, Ab7260, Abcam), anti-Iba1 antibody (1: 300, CP 290 A, Biocare Medical), and anti-Parvalbumin antibody (1:500, Ab11427, Abcam).

Image acquisition, processing and analysis

Image acquisition is described in detail in Supplementary Fig. 1. Adobe Photoshop was used to crop the original images and to apply brightness and contrast adjustments.

Imaris version 8.3.1 (Bitplane Scientific) was used for automated cell counting and co-localization analysis. To determine co-localization of tdTomato and NeuN fluorescence, three consecutive horizontal sections at bregma −3.44 mm (Fig. 1) were used (Paxinos and Franklin, 2013). We created a region of interest that represented the slice volume based on NeuN immunoreactivity by using the Surface module. This 3D structure was used for further analyses. Five representative active cells in the lower end of the intensity spectrum were selected and their contours were drawn. Their mean intensity threshold was applied to build a co-localized image using the Coloc module. The co-localized voxels were counted and plotted as a percentage of the volume of the slice.

The number of TRAPed neurons was also counted for dentate granule cells (DGCs), piriform cortex, and entorhinal cortex. For each structure, the region of interest was marked. Based on intensity, we identified both NeuN and tdTomato-positive cells using the Spots module. The number of tdTomato spots that overlapped with the NeuN spots corresponded to the number of TRAPed neurons. The investigator analysing the co-localized voxels or the number of TRAPed neurons was blinded to the time of 4-OHT administration.

Statistical analysis

The data are represented as the mean ± standard error of the mean (SEM) and were compared using one-way ANOVA followed by *post hoc* Dunnett's multiple comparison test. Comparison between two groups was performed using Student's *t*-test. The data on time course of neuronal activation were fitted to either an equation for a Gaussian or a straight line. All statistical analyses were performed using GraphPad Prism software (GraphPad Software Inc.).

Data availability

The data that support the findings of this study are available from the corresponding author, upon reasonable request.

Results

Overview of seizure spread during status epilepticus

Electrical stimulation of the hippocampus initially caused stimulus train-locked seizures, which over time became stimulus-independent and continued for 1.5–5 h after the end of stimulation (Supplementary Fig. 1B) (Lewczuk *et al.*, 2018). Behavioural seizures increased in severity after the end of stimulation, reaching a peak at 60–120 min from the beginning of stimulation (T0 + 60 − 120). During this time period, recurrent Racine grade 4–5 seizures (Racine, 1972) were observed and were accompanied by high amplitude fast discharges on EEG and spikes of increased power on the compressed spectral display of the EEG. After reaching a peak, severe seizures became less frequent, and the frequency of spike wave discharges slowed. The original characterization of TRAP mice demonstrated that neurons active during 1–2 h prior to 4-OHT administration were TRAPed (Guenthner *et al.*, 2013). To TRAP neurons activated during every hour of status epilepticus, different groups of animals were injected with 50 mg/kg 4-OHT (subcutaneously) at 60, 120, 180, 240 and 300 min after starting hippocampal stimulation (Supplementary Fig. 1A).

To obtain an overview of the brain structures activated during the course of status epilepticus, sections at the level of the olfactory bulb (bregma −3.44, Plate 148) (Paxinos and Franklin, 2013) from animals at T0, T0 + 60, +120, +180, +240 and +300 min from start of stimulation were examined (Fig. 1A). Each section was counterstained with NeuN to clearly distinguish neurons from non-neuronal cells, which may also express tdTomato. We considered TRAPed neurons as those cells that expressed both tdTomato fluorescence and NeuN immunoreactivity. When 4-OHT was administered without any stimulation (T0), tdTomato fluorescence was present around the electrode (Fig. 1A) and in scattered neurons in the hippocampus, thalamus and somatosensory cortex.

In slices from animals injected at T0 + 60, tdTomato fluorescence was observed in the dentate gyrus, CA1, CA2 and CA3 regions of the hippocampus, subiculum, pre- and parasubiculum bilaterally, and in the lateral entorhinal cortex. tdTomato fluorescence was also visible over both fimbria-fornix, which connect the hippocampus to the septum, where TRAPed neurons were present in the lateral septal nucleus. In addition, there was tdTomato fluorescence in the olfactory bulb, internal and external plexiform layer, and the granule cell layer of the olfactory bulb, which receives direct inputs from the lateral entorhinal cortex.

In the time period following hippocampal stimulation (T0 + 60 − 120 min) Racine grade 4 or 5 seizures occurred intermittently on a background of grade 2 seizures. A compressed spectral display of the EEG obtained in the 90 min prior to 4-OHT from the animals in Fig. 1A display several high power peaks (Fig. 1C), which were associated with Racine grade 4 or 5 seizures. When animals were injected at T0 + 120, fluorescence was more intense in the structures that were active at T0 + 60; in addition, neurons in a larger set of structures were TRAPed. There was tdTomato fluorescence in the outputs of the olfactory bulb; the anterior olfactory cortex (ventral and medial), piriform cortex and entorhinal cortex. tdTomato fluorescence was present over neocortical structures; the insular cortex, agranular cortex, ectorhinal cortex and perirhinal cortex. In dorsal sections, targets of the cingulate cortex; the motor and supplementary motor cortex, somatosensory cortex and association areas of the cortex were activated. In addition, the amygdala and midline thalamus also

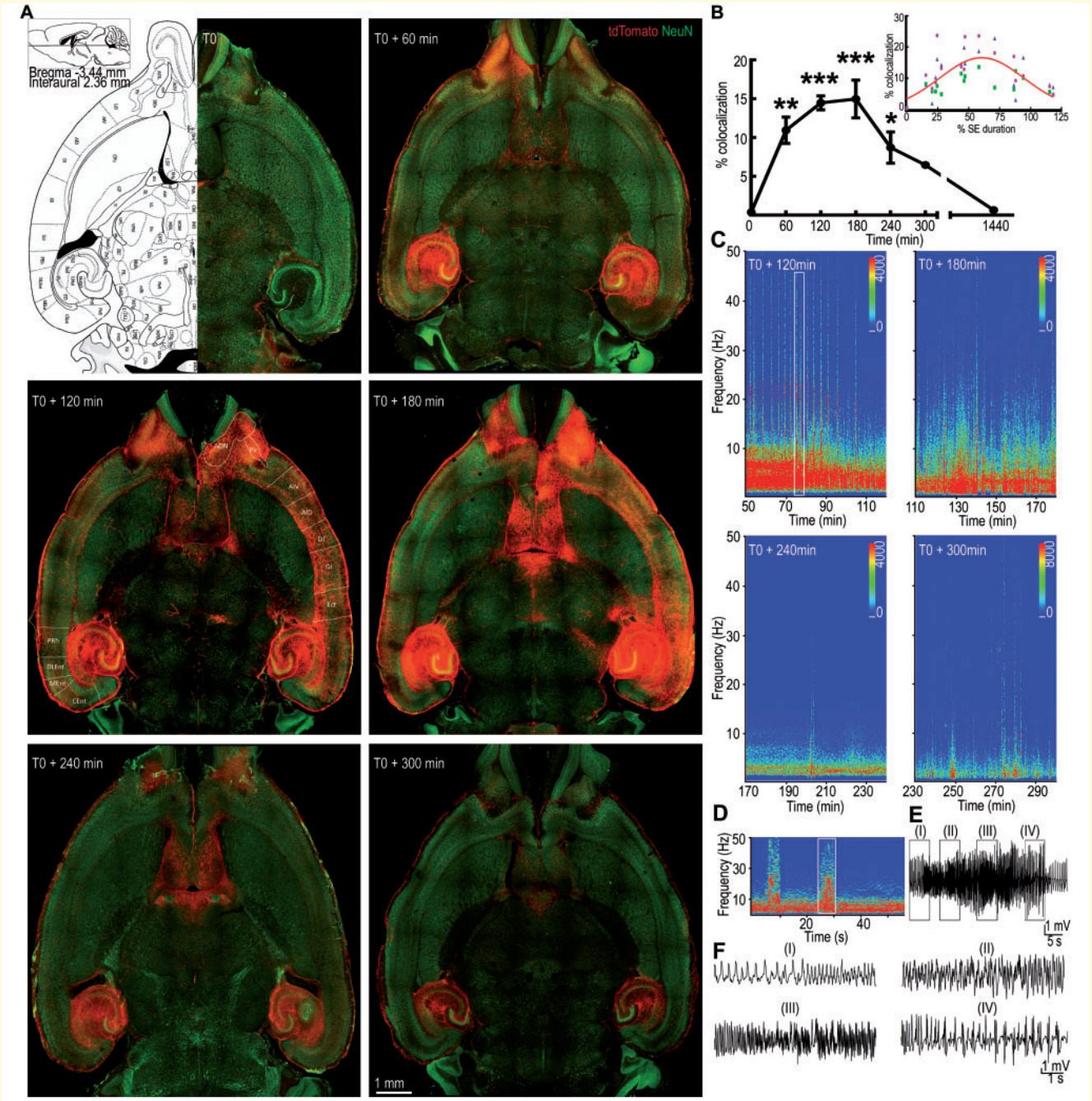

Figure 1 The pattern of neuronal activation during status epilepticus. (**A**) Horizontal brain sections from animals injected with 4-OHT at different times from the start of continuous hippocampal stimulation (T0). A plate from the Paxinos mouse atlas at the level of the displayed sections is shown for comparison. The tdTomato fluorescence (red) corresponds to TRAPed cells and NeuN immunoreactivity (green) labels the neurons. Regions containing tdTomato-labelled neurons are marked as follows: AON = anterior olfactory nucleus; Pir = piriform cortex; AIV and AID = ventral and dorsal parts of agranular insular cortex, respectively; DI = dysgranular insular cortex; GI = granular insular cortex; Ect = ectorhinal cortex; PRh = perirhinal cortex; DLEnt, MEnt and CEnt = dorsolateral, medial and caudomedial entorhinal cortex, respectively. (**B**) The tdTomato voxels co-localized with NeuN immunoreactivity are expressed relative to that at T0. The values represent mean ± SEM of co-localized voxels from three consecutive 200-μm thick slices for each animal; $n = 5$ for T0 + 60 and $n = 3$ for T0, T0 + 120, +180, +240, +300 min and +24 h. *$P < 0.05$, **$P < 0.005$, ***$P < 0.0005$ versus T0, ANOVA with *post hoc* Dunnett's multiple comparison test. The *inset* shows the co-localized voxels plotted against the time of 4-OHT administration normalized to the total duration of status epilepticus in each animal. The voxels from each of the three sections used for quantification are plotted separately in three colours. (**C**) Spectrograms show the power of the EEGs recorded from the hippocampal electrodes during 90 min prior to 4-OHT administration. This activity corresponds to the neuronal TRAPing captured in the images in **A**. (**D**) Power spectrum magnified from the boxed region in **C**, which corresponds to a tonic-clonic seizure. (**E**) A high amplitude fast spike-wave discharge on EEG corresponding to the band of high power marked by the box in **D**. (**F**) Magnified EEG, corresponding to regions (I), (II), (III) and (IV) in **E**. SE = status epilepticus.

contained TRAPed neurons. Injections at T0 + 180 were preceded by multiple Racine grade 4 or 5 (generalized tonic-clonic) seizures and spikes of increased power on the compressed spectral displays of the EEG. In images obtained from animals injected at T0 + 180, the tdTomato fluorescence was observed in structures also activated at T0 + 120.

The waning phase of status epilepticus is characterized by milder seizures (Racine grade 2 and 1), diminishing occurrence of high amplitude fast discharges (Fig. 1D–F), and slowing frequency of high amplitude slow discharges on EEG (Fig. 1C). Based on the previously reported duration of status epilepticus, 4-OHT was administered 240 or 300 min after the onset of stimulation to assess the waning phase of status epilepticus. Our overall impression of the whole brain sections was a recession of a recently crested wave. Neurons TRAPed at the initiation of status epilepticus were also TRAPed in the waning phase of status epilepticus. At T0 + 240 min, the TRAPed neurons were again restricted to the hippocampi, septum and olfactory bulbs, similar to that seen at T0 + 60 min (Fig. 1A). To determine whether the neuronal TRAPing returned to the baseline after seizures have ended, a cohort of animals was treated with 4-OHT at T0 + 24 h. In these animals few TRAPed neurons were present in the dentate gyrus, CA1, septum and entorhinal cortex of the ipsilateral hemisphere (Supplementary Fig. 7A).

We then analysed images from horizontal and coronal sections of the entire brains of animals injected with 4-OHT at T0 and T0 + 60, +120, +180, +240 and +300 min time points to delineate the neuronal circuits that were active during various stages of status epilepticus (Supplementary Figs 2–6). Visual examination of the sections obtained from animals at various time points during status epilepticus suggested TRAPed neurons occupied larger volumes of the brain as the seizures progressed in a wave-like fashion from the hippocampus to the neocortex and then recessed. A large fraction of tdTomato-expressing neurons were observed in the ventral part of the brain encompassing the hippocampus, entorhinal, ectorhinal, insular and piriform cortex, midline septum, olfactory nucleus, olfactory bulbs, and the thalamus.

We quantitatively assessed the volume of tdTomato fluorescence as a fraction of Alexa Fluor® 488 fluorescence (NeuN) in three horizontal sections (200 µm) from animals injected at T0 ($n = 3$), T0 + 60 ($n = 5$), T0 + 120 ($n = 3$), T0 + 180 ($n = 3$) T0 + 240 ($n = 4$), T0 + 300 ($n = 3$), and T0 + 24 h ($n = 3$). Consistent with the visual impression, the volume of tdTomato fluorescence as a fraction of NeuN fluorescence increased as a function of time after administration of 4-OHT, reaching a peak at T0 + 180 and then receding to baseline over the next 120 min (Fig. 1B). However, the end of status epilepticus is a variable process, with the duration of status epilepticus ranging from 89 to 371 min (median 256 min, $n = 20$). To understand the waning phase of status epilepticus, the time of administration of 4-OHT was normalized to the duration of status epilepticus in each animal. As illustrated in Fig. 1B, the data were best fit to a Gaussian curve; the percentage of neuronal trapping was low at the beginning of status epilepticus, it increased to a peak of 16–18% at the middle of status epilepticus and subsequently declined as seizures waned. These time course studies demonstrated that maximal neocortical activation was observed in the brains of mice injected at T0 + 120 and T0 + 180 min. In this status epilepticus model, severe motor seizures occur between T0 + 60 and T0 + 120, which is 60–120 min prior to the injection of 4-OHT. This suggested that the latency between seizures and appearance of TRAPed neurons is 60–120 min, which is consistent with the original characterization of these animals.

We confirmed that neuronal activation maps obtained by the TRAP method were similar to those obtained by immunohistochemistry for endogenous cFos. In a cohort of C57Bl/6 mice, status epilepticus was induced by continuous hippocampal stimulation and after 2 h of self-sustaining seizure activity (T0 + 180), immunohistochemistry for cFos was performed. Endogenous cFos immunoreactivity was observed in the DGCs, lateral septum, and olfactory bulbs (Fig. 2A). This was similar to the pattern of tdTomato fluorescence observed in the sections from TRAP mice in status epilepticus (Fig. 2B).

Motor cortex activation

Motor cortex activation was best observed in animals injected at T0 + 120 and T0 + 180 min. For the current study, the motor cortex was defined as the lateral part of the frontal cortex from 2.6 mm anterior to the bregma through the bregma in the coronal sections. In sections obtained from animals at T0 + 120, there was intense and widespread TRAPing of neurons in the superficial layers in the primary and secondary motor cortex, and less intense activation of deeper layer neurons (Fig. 3A). More intense activation was observed in more rostral sections (Fig. 3A) and it diminished in intensity in the rostrocaudal direction (Fig. 3A). As the motor cortex has rich interconnections with the somatosensory cortex, we also obtained high magnification images of the somatosensory cortex (Fig. 3B). Superficial layers of the somatosensory cortex receive projections from motor cortex and send projections to superficial layers of motor cortex. Consistent with the known cortical connectivity, TRAPed neurons were most commonly found in the superficial layers of the cortex in the early phases of status epilepticus. There was greater TRAPing of neurons in the superficial layers at the peak of status epilepticus and activation of deeper layer neurons in the infra-granular layer.

Generalized tonic-clonic seizures involve bilateral motor movements of limbs and midline axial musculature; this would suggest bilateral motor cortex activation. In horizontal sections from brains spanning the cortex of animals

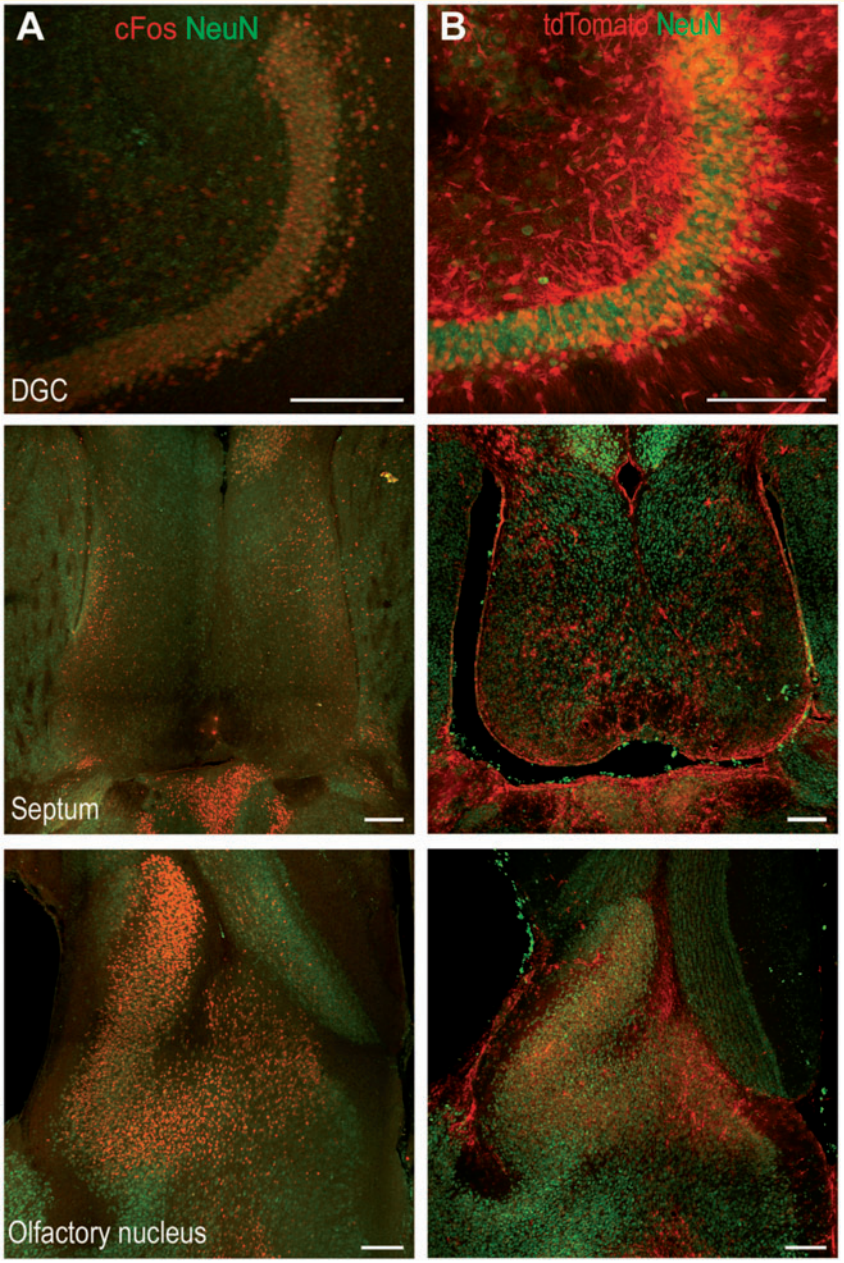

Figure 2 Similar pattern of tdTomato expression and immunoreactivity of endogenous cFos. (**A**) The immunoreactivity of cFos and NeuN in the DGCs, septum and olfactory nucleus at T0 + 180 min in a C57Bl/6 animal. (**B**) The tdTomato expression and NeuN immunoreactivity in a TRAP animal at T0 + 180 min. Scale bars = 200 μm.

injected at T0 + 120 or T0 + 180, activation was bilateral, but it was often asymmetric where one hemisphere was more active than the other. We quantified the degree of asymmetry by comparing the volume of tdTomato-expressing neurons in the more active cortex to less active cortex. In sections from 14 animals injected at T0 + 120 or T0 + 180, NeuN co-localized tdTomato fluorescence on the less activated side was 56.9 ± 7.7% (n = 14 animals, P = 0.0001, Mann-Whitney U-test) of that in the contralateral cortex.

Despite the asymmetry, there was bilateral activation of cortices. The corpus callosum extensively connects both cortices and could provide a means for seizure spread. Examination of the corpus callosum revealed tdTomato-filled fibres, especially in animals with extensive bilateral activation (Fig. 3C). Layer II neurons send out cortico-cortical projections to the contralateral cortex via the corpus callosum (Weiler *et al.*, 2008). Bilateral superficial cortical activation and tdTomato-filled corpus callosum were observed in several animals.

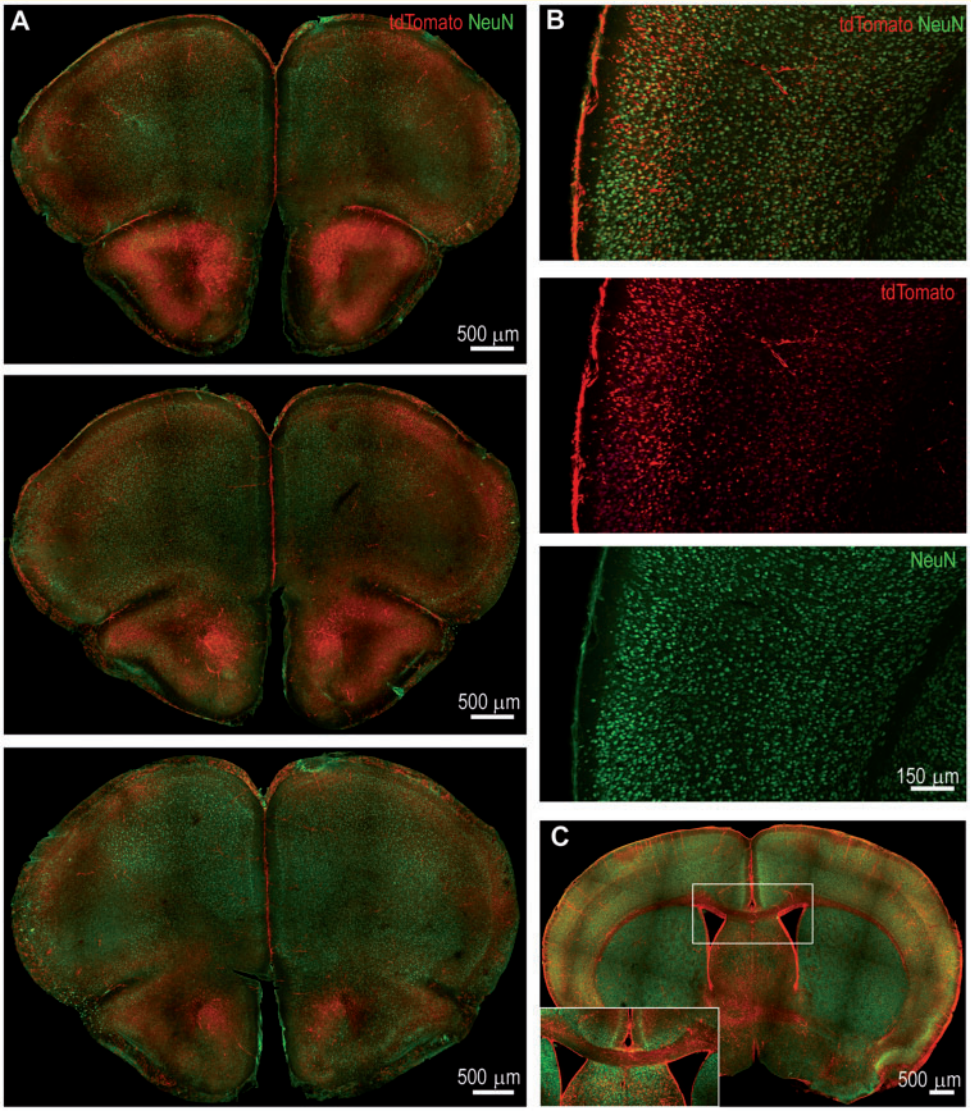

Figure 3 Neurons in the superficial layers of the motor and somatosensory cortex were TRAPed at the peak of status epilepticus. (**A**) Coronal sections from an animal at bregma 2.57 mm, 2.45 mm, and 1.97 mm (*top* to *bottom*) illustrate bilateral neuronal activation in the motor cortex at T0 + 120 min. The activation was more robust in rostral sections than in caudal sections. (**B**) Neuronal TRAPing in the somatosensory cortex at T0 + 120 min in a section at the level of bregma 0.01 mm. There was intense tdTomato expression in the superficial layers compared to the deep layers. (**C**) A coronal section at T0 + 120 min illustrating bilateral cortical activation and prominent labelling of the corpus callosum. The corpus callosum is magnified in the *inset* and shows tdTomato-filled axons, which originate in layer II/III of the cortex.

Prominent activation of the superficial layers of the cortex suggested that seizures could be spreading via intratelencephalic projections. The motor cortex receives rich connections from other neocortical areas; somatosensory cortex, visual, auditory and associational cortex. In addition, it also receives inputs from motor thalamic nuclei such as anterior thalamic nucleus, ventrolateral thalamic nucleus, and ventromedial thalamic nucleus (Kuramoto *et al.*, 2009; Hooks *et al.*, 2013). Current models of secondary generalization of seizures propose that seizures spread through thalamocortical oscillations. We examined activation of the motor thalamic nuclei during peak status epilepticus.

Motor, midline, reticular and posterior thalamic nuclei were activated

Several motor thalamic nuclei contained TRAPed neurons indicative of their activation at the peak of status epilepticus (Fig. 4). Intense tdTomato labelling was present in the

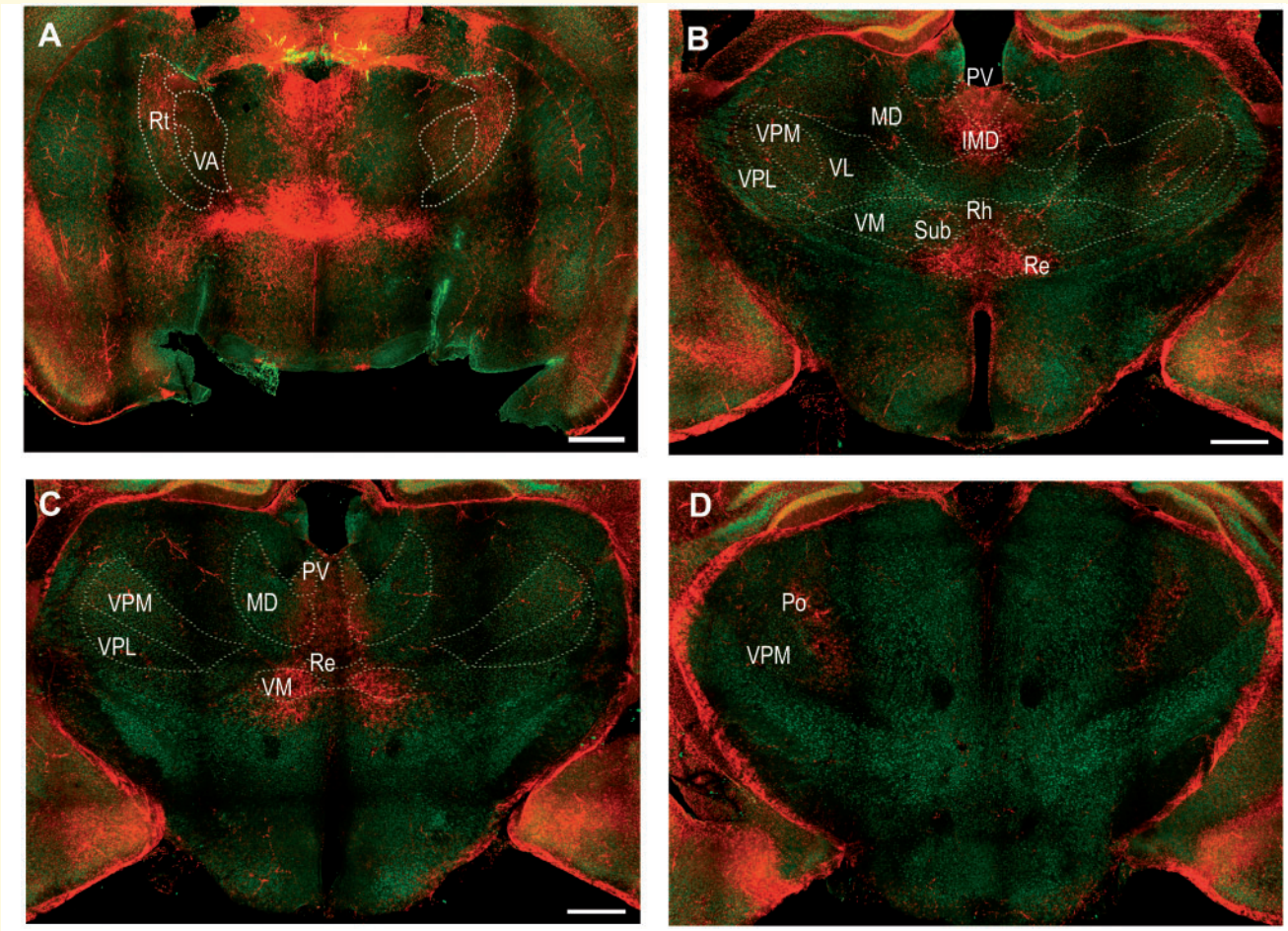

Figure 4 Activation of the motor, midline, reticular and posterior thalamic nuclei at the peak of status epilepticus. Coronal sections at the level of bregma −0.83, −1.43, −1.91 and −2.53 mm (**A** to **D**, respectively) indicating activation of motor thalamic nuclei: ventromedial (VM) and ventral anterior (VA); midline thalamic nuclei: mediodorsal (MD), paraventricular (PV), intermedio-dorsal (IMD), rhomboid (Rh), reuniens (Re), and submedius (Sub). Other areas marked include reticular nucleus (Rt) and posterior complex of thalamus (Po), which also contained TRAPed neurons. Motor thalamic nucleus (VL) as well as sensory thalamic nuclei ventral posteromedial (VPM) and ventral posterolateral (VPL) had sparse tdTomato labelling.

ventromedial thalamic nucleus (Fig. 4) and TRAPed neurons were also present in the anterior thalamic nucleus (Fig. 4). However, tdTomato labelling was sparse in the ventrolateral thalamic nucleus.

In addition to motor thalamic areas, midline thalamic nuclei, some of which project to the somatosensory cortex, were also activated at the peak of status epilepticus (Fig. 4). There was prominent activation of paraventricular, mediodorsal nucleus, intermediodorsal, rhomboid, reuniens, and submedius thalamic nuclei (Fig. 4). The activation was most consistent in the anterior thalamus (Fig. 4). In addition, TRAPed neurons were also present in the reticular thalamus and posterior complex of the thalamus, both of which have connections to the somatosensory cortex (Fig. 4). In contrast, ventroposterior medial and ventroposterior lateral thalamic nuclei, which also project to the somatosensory cortex, were marked by limited tdTomato fluorescence (Fig. 4).

Seizure spread to the motor cortex during status epilepticus may occur through midline thalamus and through anterior and ventromedial thalamic nucleus, which were activated. An alternate route of seizure spread could involve the pathway of memory consolidation. Therefore, we determined whether components of memory engram including entorhinal cortex, retrosplenial cortex, cingulate cortex, and reunions nucleus were activated during status epilepticus in the subsequent studies. According to the online mouse connectome provided by the Allen Institute (Oh *et al.*, 2014) (http://connectivity.brain-map.org/) and published literature, these regions are also interconnected with each other and with hippocampus and can propagate the activity in an efficient manner.

Cingulate gyrus, insular cortex and olfactory system

During peak status epilepticus intense tdTomato fluorescence was observed over the insular cortex and cingulate cortex (Fig. 5C and E). Neurons expressing tdTomato were present in the cingulate cortex at T0 + 60 min; their density appeared to be more in the caudal part of the cingulate gyrus and more in the sections encompassing the septum than in the rostral sections at the level of the motor cortex. There were many TRAPed neurons in the superficial layers of the cingulate gyrus (Fig. 5C). The tdTomato fluorescence declined during the waning phase of status epilepticus. The caudal region of the cingulate cortex (bregma −0.95 mm to −4.35 mm) constitutes the retrosplenial cortex (Sugar *et al.*, 2011; Oh *et al.*, 2014; Yamawaki *et al.*, 2018). It receives afferents from the dorsal hippocampus and parahippocampal structures (Cenquizca *et al.*, 2007) and forms reciprocal monosynaptic excitatory connections with the pyramidal neurons of the secondary motor cortex (Yamawaki *et al.*, 2018). In addition, there are disynaptic projections between the motor cortex and retrosplenial cortex via the anteromedial thalamus. Thus, these neurons are positioned to relay information between the hippocampus and neocortical networks. Assessment of this region revealed the presence of TRAPed neurons (Fig. 5E). There was extensive labelling of superficial layer neurons at T0 + 120 and T0 + 180 min. The activation of neurons was always bilateral and appeared to be more prominent rostrally than caudally.

The insular cortex serves as a hub between cortical areas and it was intensely activated during status epilepticus. For this study, we defined the insular cortex as the region bounded superiorly by the motor and somatosensory cortex, and inferiorly by the piriform cortex, posteriorly by the ectorhinal and perirhinal cortices and anteriorly by the orbital cortex (Gogolla, 2017). In both coronal and horizontal sections, the pattern of tdTomato fluorescence over the insular cortex showed intense labelling of neurons in the superficial layer, with sparser labelling of deeper layers (Fig. 5D and F). Insular cortex labelling was contiguous with the piriform cortex labelling in the horizontal and coronal sections.

The piriform cortex, which projects to the insular cortex and receives direct inputs from the olfactory bulb and entorhinal cortex, was the most prominently activated structure in the olfactory cortex (Fig. 5D and F). There was intense tdTomato fluorescence in both the posterior and anterior (dorsal and ventral) piriform cortex in horizontal and coronal sections. In addition, intense tdTomato fluorescence was present over the ventrorostral aspect of piriform cortex, which is referred to as the area tempesta in the epilepsy literature (Piredda and Gale, 1985). TRAPed superficial neurons and diffuse low level tdTomato fluorescence was observed in the outer, plexiform layer (layer I). Much more widespread and intense staining was present in the compact cell layer (layer II). Neurons in both the superficial and deeper layer II were TRAPed. There is a gradient of cells from the superficial to deeper parts of layer III of the piriform cortex, which are interspersed with axon bundles. Several TRAPed neurons were observed in this layer. Deeper in layer III, many TRAPed neurons were observed in the endopiriform nucleus, which is also referred to as layer IV of the piriform cortex.

There was bilateral activation of the piriform cortex, anterior olfactory nucleus, and olfactory bulbs, which are connected by the anterior commissure. Many fibres in the anterior commissure originate from layer II of the anterior part of the piriform cortex and terminate on the contralateral side of the posterior part of the piriform cortex and adjacent olfactory cortical areas (Haberly and Price, 1978). There was intense tdTomato fluorescence in the anterior commissure, where high resolution images showed individual axons filled with tdTomato (Fig. 5D). TRAPed neurons were present in several amygdala nuclei (Supplementary Fig. 5). Similarly, the perirhinal cortex and ectorhinal cortex were also activated (Supplementary Figs 3 and 4).

Activation of the olfactory bulbs was observed in animals injected with 4-OHT early in status epilepticus, at the peak status epilepticus, and during the waning phase of status epilepticus (Fig. 5A and Supplementary Figs 2–6). The olfactory bulb receives direct inputs from the ventral hippocampus (CA1 pyramidal neurons and subiculum) and lateral entorhinal cortex, both of which were activated during early status epilepticus (Mohedano-Moriano *et al.*, 2012). The fluorescence was often observed most intensely in the granule cell layer, less intensely in the glomerular layer and external plexiform layer, and occasionally in the mitral cell layer (Fig. 5A). More caudally at the level of the anterior commissure, intense labelling of neurons in the granule cell layer was present, with limited tdTomato fluorescence in the external plexiform layer (Fig. 5B). In addition, the anterior olfactory nucleus demonstrated tdTomato fluorescence. Outputs of the olfactory bulb: piriform cortex, entorhinal cortex, agranular insular cortex, amygdala complex, midline thalamic nuclei, and olfactory peduncle expressed tdTomato fluorescence.

Hippocampus and parahippocampal circuit

The olfactory system, associational insular cortex and the neocortex receive inputs from the hippocampus and parahippocampal structures: subiculum and entorhinal cortex. We first examined the activation of the entorhinal cortex. A striking feature of entorhinal cortex activation was that the lateral entorhinal cortex was activated more intensely and persistently than the medial entorhinal cortex (Fig. 6A and E). Within the lateral entorhinal cortex, TRAPed neurons were present in the superficial layers of sections obtained from T0 + 60 animals. It is likely that intense activation of the hippocampus resulted from re-entrant seizure activity since layer II/III entorhinal cortex neurons project to

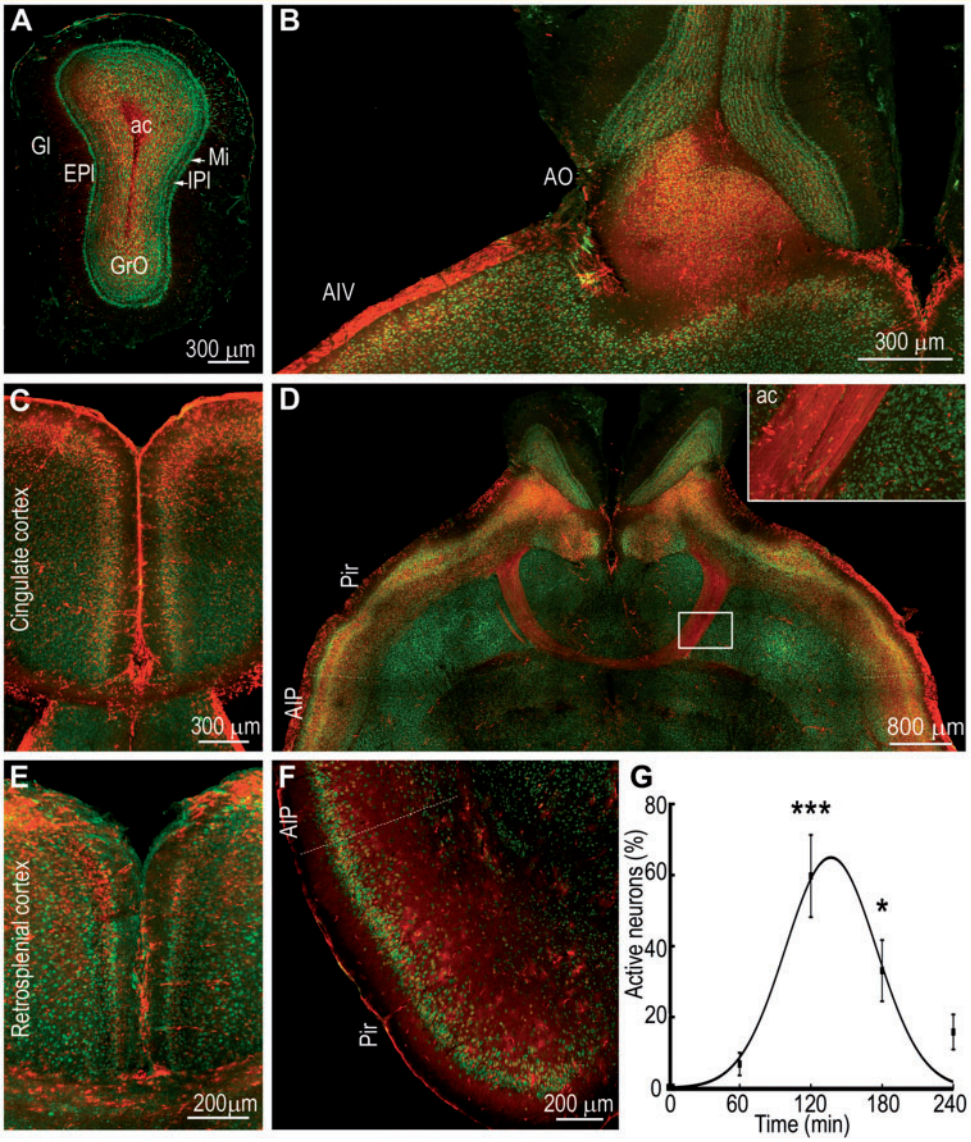

Figure 5 Intense activation of the olfactory system during status epilepticus. (**A**) A section through the olfactory bulb showing intense activation of granule cells (GrO) and little activation of the neurons in the glomerular layer (GI) and external plexiform layer (EPl) at T0 + 120 min. Other areas marked are the internal plexiform layer (IPl), mitral cell layer (Ml), and anterior commissure (ac). (**B**) An image showing strong activation of the olfactory nucleus (AO) and ventral agranular insular cortex (AIV). (**C**) A section showing TRAPed neurons in the superficial layers of cingulate cortex. (**D**) A horizontal section showing the anterior commissure (ac) with axons filled with tdTomato fluorescence joining the two hemispheres containing TRAPed neurons in the piriform cortex (Pir) and posterior agranular insular cortex (AIP). The *inset* shows a magnified region of the ac. (**E**) An image showing bilateral activation of neurons of the superior layers of the retrosplenial cortex. (**F**) Extensive TRAPing of the neurons of the posterior agranular insular cortex and piriform cortex is also visible in a section in the coronal orientation. (**G**) The number of TRAPed neurons in the piriform cortex were counted in one 10-µm thick optical section and plotted against time; $n = 3$ each at T0, T0 + 60, +120 and +180 and $n = 2$ at +240 min. ***$P < 0.0005$ and *$P < 0.05$ versus T0, ANOVA with Dunnett's multiple comparison test. The line shows the fit of the data to a Gaussian curve.

DGCs, which propagate activity to the rest of the hippocampus and allow the hippocampus to feed back to the entorhinal cortex via subiculum. The activity becomes continuous and independent of electrical stimuli on EEG during the 60-min time period. At the peak of status epilepticus, neurons in both the superficial and deeper layers of the entorhinal cortex were TRAPed, which were mixed with astrocytes expressing tdTomato.

There was intense tdTomato fluorescence in the stimulated and contralateral hippocampus, and in the lateral septum. In the hippocampus, the components of the trisynaptic pathway: DGCs that gate input, CA3 pyramidal neurons, and CA1 pyramidal neurons were TRAPed (Fig. 7A). In contrast to the cortical structures, the hippocampus was active throughout the course of status epilepticus. As DGCs are proposed to gate neuronal activity, we

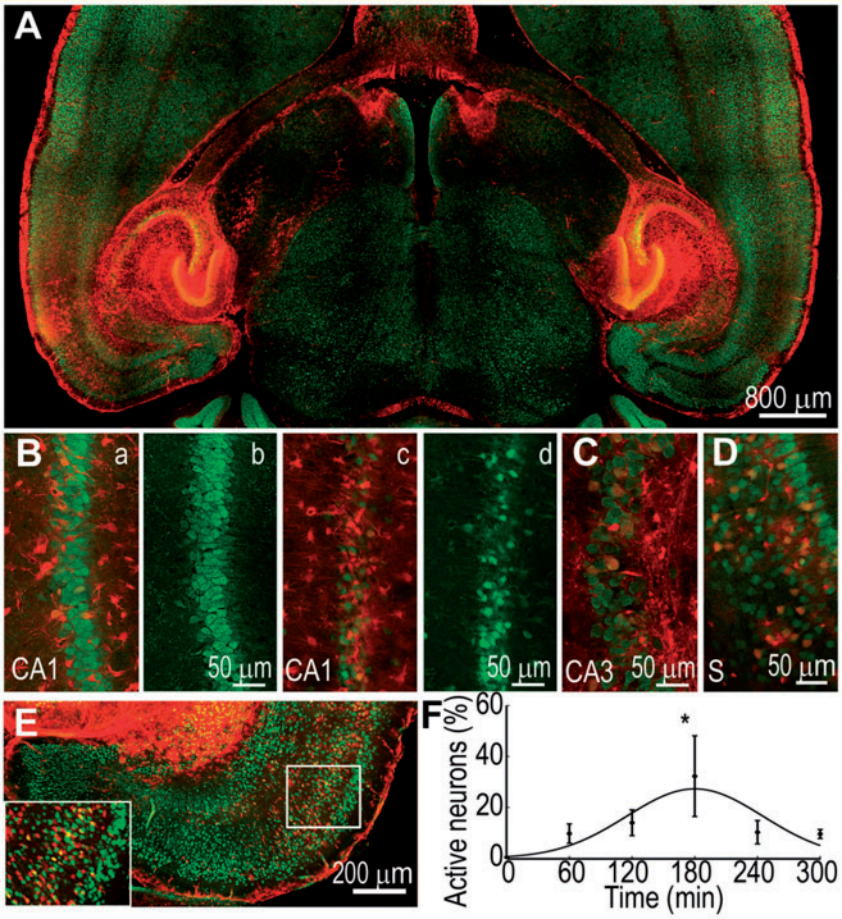

Figure 6 TRAPing of neurons in the hippocampus and its outputs. (**A**) A horizontal section showing bilateral activation of the hippocampi and hippocampal outputs; subiculum, parasubiculum, lateral entorhinal cortex, and septum. Fimbria filled with tdTomato is visible, connecting hippocampi to septum. (**B**) Activation of CA1 pyramidal neurons in two animals revealed by co-localization of tdTomato and NeuN (**a** and **c**). Images in **b** and **d** show NeuN immunoreactivity alone to illustrate extensive neurodegeneration in the second animal (**d**) compared to that in the first animal (**b**). (**C** and **D**) CA3 and subiculum containing TRAPed neurons. (**E**) A section showing activation of neurons in the superficial and deeper layers of the lateral entorhinal cortex. Please note the absence of TRAPed neurons in the medial entorhinal cortex. (**F**) tdTomato labelled neurons were counted in the entorhinal cortex from one 10-µm thick optical section from each animal; $n = 3$ each for T0, T0 + 60, +180, +300, $n = 4$ for T0 + 120, and $n = 2$ for T0 + 240 min. *$P < 0.05$ versus T0, ANOVA with Dunnett's multiple comparison test. The line shows that the activation was explained by a Gaussian fit.

evaluated their activation through the course of status epilepticus. Starting at T0 + 60, there was bilateral and substantial TRAPing of DGCs (Fig. 6A) and this level of activation was mostly maintained throughout status epilepticus (Fig. 7A). TRAPed neurons were spread over the entire dentate along the septo-temporal axis of the hippocampus (Supplementary Figs 2–6). We counted the number of TRAPed DGCs using high magnification images; only 0.1% of DGCs were active at T0, and this fraction increased to 29 ± 7% at T0 + 60 min ($n = 3$) and remained steady until T0 + 300 min (28 ± 7%, $n = 3$; Fig. 7C). Thus, there was a sharp increase in the activation of the DGCs at T0 + 60 min, and once the DGCs were activated, their activation level was maintained even at T0 + 300 min (Fig. 7C). A linear regression line best described the activation of the DGCs during status epilepticus; the slope of this line was close to 0 (0.006; Fig. 7C) and the *y*-intercept was 28.7. The observed sudden increase was followed by a steady level of activation of the DGCs and was in agreement with current theories that the dentate acts as a gate.

As a substantial fraction of the DGCs remained active at T0 + 300 min, we determined whether the activity had decreased to the baseline level at T0 + 24 h. At this time, the number of TRAPed DCGs had decreased, but it still remained higher than that at the baseline (0.85%; Supplementary Fig. 7).

Discussion

In this study, active neurons of the entire forebrain were imaged in an unbiased fashion at multiple time points,

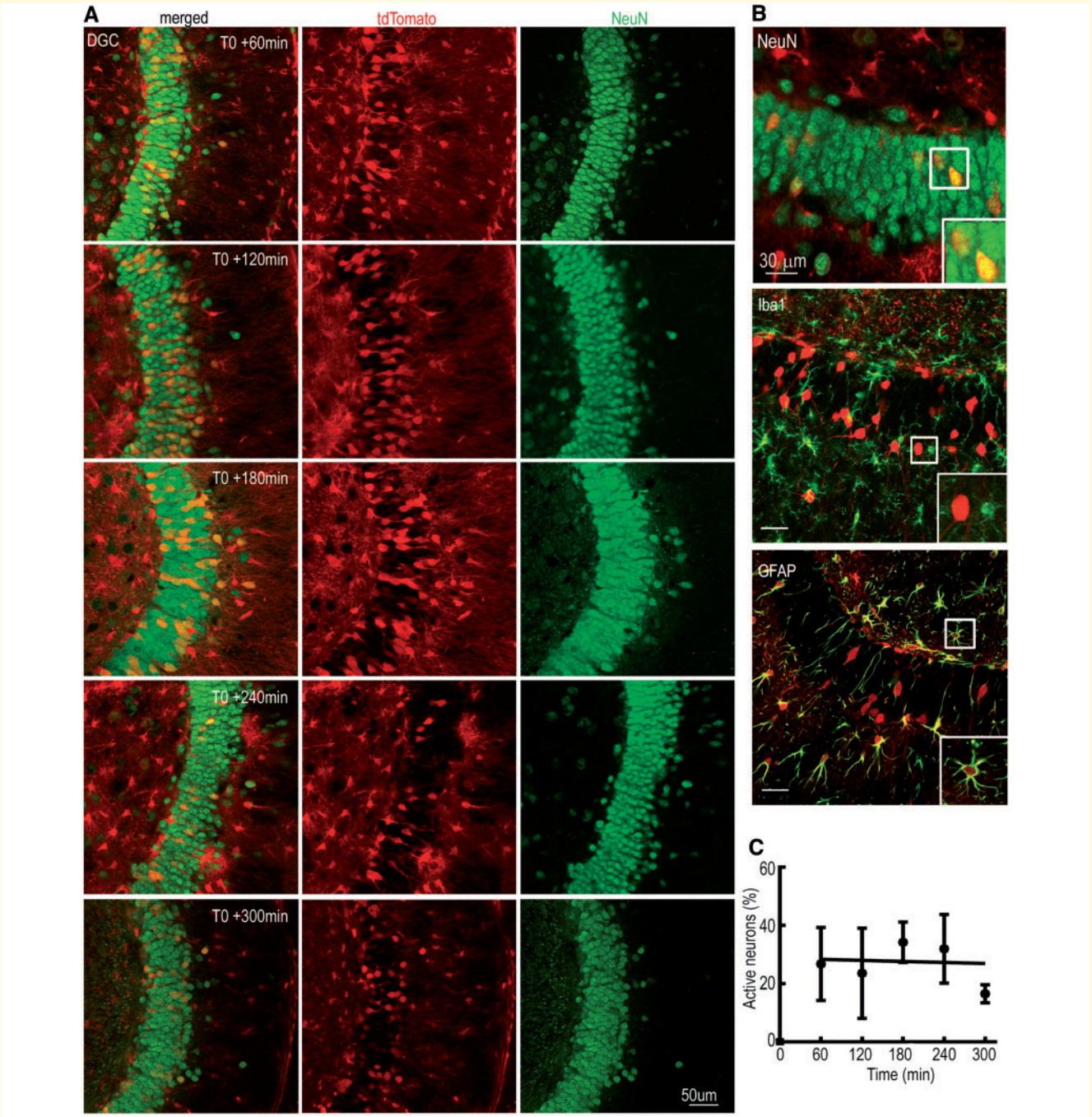

Figure 7 DGC activation during the course of status epilepticus. (**A**) TRAPing of DGCs at T0 + 60 to T0 + 300 min. (**B**) Co-localization of TRAPed neurons in the dentate gyrus with the neuronal marker protein NeuN, microglial marker protein Iba1 and astrocyte marker protein GFAP. The *insets* show boxed areas in the respective image. (**C**) The number of activated DGCs was plotted over time; $n = 3$ each for T0, T0 + 60, +120, +180, $n = 4$ for T0 + 240 and $n = 2$ for T0 + 300. The line depicts a linear regression fit of the data.

allowing us to visualize the activation of the motor cortex and other areas during peak seizure activity. Motor, midline, reticular and posterior thalamic nuclei were activated during status epilepticus, in addition to hippocampus and olfactory system. The midline thalamic nuclei project to the medial prefrontal cortex and diffusely to the cortex (Vertes *et al.*, 2015), whereas, motor thalamic nuclei such as anterior thalamic nucleus and ventromedial thalamic nucleus project to layers I–V and I and II/III neurons of the motor cortex, respectively (Hioki *et al.*, 2013). Neurons were also active in cortico-cortical pathways connecting the hippocampus to the motor cortex: including entorhinal cortex, retrosplenial cortex, cingulate gyrus, and midline thalamic nuclei. Many of these structures are intimately

involved in memory consolidation and retrieval (Kitamura *et al.*, 2017).

TRAP mice were advantageous over the detection of endogenous expression of immediate early gene (IEG) protein or mRNA expression. The increase in endogenous cFos expression is small and transient. This increase was amplified by the use of bright fluorescence of tdTomato and by its permanence; tdTomato expression once triggered never switches off. Thus, there was improved signal-to-noise ratio, which allowed for high resolution imaging of single cells. In addition, the coupling of Cre recombinase with ER provided additional temporal resolution of 60–90 min. Making use of these improvements we found intense activation of cortical structures as well as that of the neurons of midline thalamus and motor thalamus including ventromedial thalamic nucleus and anterior thalamic nucleus at the peak of status epilepticus, when generalized seizures were common (Vertes *et al.*, 2015). In contrast, there was limited activation of ventrolateral thalamic nucleus, which also projects to the motor cortex. The absence of TRAPed neurons in the ventrolateral thalamic nucleus could be because this nucleus was not activated during status epilepticus or the technique used was inadequate to detect its activation. Neuronal TRAPing was dependent on the dynamics of cFos expression in response to neuronal activity; it is possible that the cFos promoter is less sensitive to neuronal activity in thalamic nuclei. Furthermore, intensity of labelling may also be influenced by neuronal density. Additional electrophysiological studies are needed to evaluate whether the areas that were devoid of TRAPed neurons did not experience seizure activity.

The current model of secondary generalization of seizures proposes that they spread from limbic structures or the neocortex to the thalamus and then generalize via subcortical circuits (Westbrook, 2000; Schindler *et al.*, 2007; Peng and Hsin, 2017). Subcortical thalamic circuits similar to those involved in generating generalized absence seizures have been proposed to play a role in secondarily generalized seizures, reinforcing the canonical model (Blumenfeld *et al.*, 2009*b*). In the classical view of seizure generalization, the subcortical centrencephalic integrating system, which includes the thalamus and brainstem structures, serves to coordinate and integrate the activities of two hemispheres (Jasper, 1991; Gale, 1992). Many of the areas proposed in this model of seizure generalization were activated during status epilepticus and could have contributed to seizure generalization. In addition, the intense activation of superficial cortical layers and bright labelling of corpus callosum suggests alternate parallel pathways involving cortico-cortical seizure spread may also be involved.

Corpus callosum, which bilaterally connects layer II/III neurons of the motor cortex was prominently labelled with tdTomato. There was evidence of cortico-cortical seizure spread during status epilepticus; prominent activation of the cortical inputs to the motor cortex; activation of the superficial layers of the cortex, which contain neurons connecting to different cortical areas and form the commissural tracks; and extensive tdTomato labelling of commissural fibres in the corpus callosum and anterior commissure. Superficial layers of the cortex, which contain intratelencephalic projection neurons and axons in the corpus callosum, were intensely activated during status epilepticus. Previous studies on cortico-cortical seizure spread have emphasized the role of deeper layers of the cortex in the generation and propagation of seizures (Connors *et al.*, 2001). Layer V pyramidal neurons have a low threshold for generating epileptiform bursts (Connors, 1984). In cortical slices, lateral spread of epileptiform activity was inhibited when deeper cortical layers were sectioned but not the superficial layers (Telfeian and Connors, 1998). However, a recent study using two photon microscopy to visualize the spread of seizures *in vivo* has also found preferential activation of layer II/III neurons in a chemoconvulsant model of seizures (Wenzel *et al.*, 2017). In neocortical tissue removed from patients with refractory epilepsy, there is layer II/III-specific activation of cyclic AMP response binding protein (CREB), associated with expression of proteins involved in synaptic plasticity (Beaumont *et al.*, 2012).

This study suggested memory consolidation pathway as an alternate route for seizure spread from the hippocampus to the neocortex. Studies on epilepsy patient Henry Molaisson (Patient H.M.), who underwent bilateral anterior temporal lobectomy for treatment of seizures provided first clues about the role of the hippocampus-neocortex connectivity in rapid storage and later consolidation of memories (Preston and Eichenbaum, 2013). Multiple structures in the hippocampus-neocortex pathways, which were found to be activated in the current study, have been shown to play a role in memory formation. Entorhinal cortex, reuniens nucleus, retrosplinial cortex and insular cortex are salient examples of structures involved in memory engram circuit that were activated by seizures initiated in the hippocampus (Buzsaki, 1996; Kitamura *et al.*, 2017). Throughout the episode of status epilepticus, entorhinal cortex was activated to varying degrees. Entorhinal cortex plays a key role in transmitting processed information from the hippocampus to the neocortex, and is involved in navigation, memory and planning (Suh *et al.*, 2011; Buzsaki and Moser, 2013; Stensola and Moser, 2016). Reuniens nucleus was prominently activated during status epilepticus and it is proposed to play a role in oscillatory synchrony of the hippocampus and medial prefrontal cortex, allowing formation of spatial working memory (Griffin, 2015).

There was extensive activation of the retrosplenial cortex, which has not been reported in seizure-mapping studies in the past. However, retrosplenial cortex is well documented to play a role in memory formation (Kaboodvand *et al.*, 2018; Milczarek *et al.*, 2018). This cortical region can directly relay seizures from the hippocampus to the motor cortex. Retrosplenial cortical neurons project to cortico-cortical as well as intratelencephalic neurons of the motor

cortex; thus, activation of this region can efficiently recruit both hemispheres. Furthermore, because motor cortical neurons project to cortico-cortical neurons of the retrosplenial cortex, these two regions can form an interconnected reciprocal microcircuit.

Passage of seizures through memory circuits could disrupt encoding, storage or retrieval of memory. Patients with temporal lobe epilepsy, whose seizures often originate in the hippocampus, commonly suffer from episodic memory deficits (Bell *et al.*, 2011). Seizures often cause retrograde amnesia and it is believed that this results from interference with the process of memory consolidation (McGaugh, 2000). Physical representation of memory in the brain is in the form of an engram, a set of neurons involved in storage, consolidation and retrieval of a memory through synapse modification (Tonegawa *et al.*, 2015). Recent studies have begun to identify engram cells and circuits, and the current study demonstrates activation of these circuits by seizures (Kitamura *et al.*, 2017).

In addition to pathways involved in spatial working memory, the olfactory system including the piriform cortex and endopiriform cortex were intensely active during peak status epilepticus. The endopiriform nucleus, a large mass of multipolar cells located within the piriform cortex, plays a key role in seizure generation and propagation (Piredda and Gale, 1985; Doherty *et al.*, 2000; McGinley and Westbrook, 2013).

Sparse activation of DGCs under physiological conditions plays a role in pattern separation (GoodSmith *et al.*, 2017) and it is also proposed to gate the entry of neuronal activity into the hippocampus (Heinemann *et al.*, 1992; Lothman *et al.*, 1992; Pathak *et al.*, 2007). Breakdown of the dentate gate is observed during seizures (Krook-Magnuson *et al.*, 2015). During status epilepticus, there was early breakdown of the dentate gate, which remained open at a steady state throughout the episode. The pattern of activation of DGCs was distinct from that of the neurons of the piriform cortex and entorhinal cortex, in which there was a gradual increase in the number of activated neurons to reach a peak at the apex of status epilepticus, followed by a decline in their number during the waning phase of status epilepticus. These two distinct patterns combine to generate prolonged status epilepticus, with steady activity of the hippocampus driving cortical structures that amplify this activity.

The maps uncovered in this study could be dependent on the seizure origin in the hippocampus in this model of status epilepticus. Similar mapping studies in other models of status epilepticus would be helpful to understand whether pathways leading to recruitment of motor cortex are common in all episodes of status epilepticus. The maps of activated regions marked the potential routes of seizure spread; however, their temporal resolution is not sufficient to get insights into the direction and dynamics of seizure spread. Multi-electrode local field potential recordings from activated regions would be helpful in furthering our understanding of these parameters.

In conclusion, in this first unbiased large-scale evaluation of activity maps during status epilepticus, the canonical thalamocortical pathways as well as cortico-cortical pathways were activated. Neuronal circuits involved in the formation of enduring memory engram were activated. These findings could explain memory loss following seizures.

Acknowledgements

We acknowledge the Keck Center for Cellular Imaging for the usage of the Zeiss 780 confocal/multiphoton microscopy system (OD016446) and thank Dr Ammasi Periasamy, Director of Keck Center for Cellular Imaging for advice.

Funding

This study was supported by National Institutes of Health grants R01 NS 040337 and R01 NS 044370 to J.K.

Competing interests

The authors report no competing interests.

Supplementary material

Supplementary material is available at *Brain* online.

References

Barth AL, Gerkin RC, Dean KL. Alteration of neuronal firing properties after *in vivo* experience in a FosGFP transgenic mouse. J Neurosci 2004; 24: 6466–75.

Beaumont TL, Yao B, Shah A, Kapatos G, Loeb JA. Layer-specific CREB target gene induction in human neocortical epilepsy. J Neurosci 2012; 32: 14389–401.

Bell B, Lin JJ, Seidenberg M, Hermann B. The neurobiology of cognitive disorders in temporal lobe epilepsy. Nat Rev Neurol 2011; 7: 154.

Blumenfeld H, Levin AR, Varghese GI, Motelow JE, McNally KA, Enev M, et al. Cortical and subcortical networks in human secondarily generalized tonic–clonic seizures. Brain 2009a; 132: 999–1012.

Blumenfeld H, Varghese GI, Purcaro MJ, Motelow JE, Enev M, McNally KA, et al. Cortical and subcortical networks in human secondarily generalized tonic–clonic seizures. Brain 2009b; 132: 999–1012.

Blumenfeld H, Westerveld M, Ostroff RB, Vanderhill SD, Freeman J, Necochea A, et al. Selective frontal, parietal, and temporal networks in generalized seizures. NeuroImage 2003; 19: 1556–66.

Buzsaki G. The hippocampo-neocortical dialogue. Cereb Cortex 1996; 6: 81–92.

Buzsaki G, Moser EI. Memory, navigation and theta rhythm in the hippocampal-entorhinal system. Nat Neurosci 2013; 16: 130–8.

Cenquizca LA, Swanson LW. Spatial organization of direct hippocampal field CA1 axonal projections to the rest of the cerebral cortex. Brain Res Rev 2007; 56: 1–26.

Connors BW. Initiation of synchronized neuronal bursting in neocortex. Nature 1984; 310: 685.

Connors BW, Pinto DJ, Telfeian AE. Local pathways of seizure propagation in neocortex. Int Rev Neurobiol 2001; 45: 527–46.
Doherty J, Gale K, Eagles DA. Evoked epileptiform discharges in the rat anterior piriform cortex: generation and local propagation. Brain Res 2000; 861: 77–87.
Gale K. Subcortical structures and pathways involved in convulsive seizure generation. J Clin Neurophysiol 1992; 9: 264–77.
Garner AR, Rowland DC, Hwang SY, Baumgaertel K, Roth BL, Kentros C, et al. Generation of a synthetic memory trace. Science 2012; 335: 1513–6.
Gogolla N. The insular cortex. Curr Biol 2017; 27: R580–6.
GoodSmith D, Chen X, Wang C, Kim SH, Song H, Burgalossi A, et al. Spatial representations of granule cells and mossy cells of the dentate gyrus. Neuron 2017; 93: 677–90.
Griffin AL. Role of the thalamic nucleus reuniens in mediating interactions between the hippocampus and medial prefrontal cortex during spatial working memory. Front Syst Neurosci 2015; 9: 29.
Guenthner CJ, Miyamichi K, Yang HH, Heller HC, Luo L. Permanent genetic access to transiently active neurons via TRAP: targeted recombination in active populations. Neuron 2013; 78: 773–84.
Haberly LB, Price JL. Association and commissural fiber systems of the olfactory cortex of the rat. I. Systems originating in the piriform cortex and adjacent areas. J Comp Neurol 1978; 178: 711–40.
Handforth A, Ackermann RF. Functional [14C]2-deoxyglucose mapping of progressive states of status epilepticus induced by amygdala stimulation in rat. Brain Res 1988; 460: 94–102.
Handforth A, Treiman DM. Functional mapping of the late stages of status epilepticus in the lithium-pilocarpine model in rat: a ^{14}C-2-deoxyglucose study. Neuroscience 1995; 64: 1075–89.
Heinemann U, Beck H, Dreier JP, Ficker E, Stabel J, Zhang CL. The dentate gyrus as a regulated gate for the propagation of epileptiform activity. Epilepsy Res 1992; 7: 273–80.
Hioki H, Furuta T, Kaneko T, Unzai T, Tanaka YR, Kuramoto E, et al. Ventral medial nucleus neurons send thalamocortical afferents more widely and more preferentially to layer 1 than neurons of the ventral anterior–ventral lateral nuclear complex in the rat. Cerebral Cortex 2013; 25: 221–35.
Hooks BM, Mao T, Gutnisky DA, Yamawaki N, Svoboda K, Shepherd GMG. Organization of cortical and thalamic input to pyramidal neurons in mouse motor cortex. J Neurosci 2013; 33: 748–60.
Jasper HH. Current evaluation of the concepts of centrecephalic and corticoreticular seizures. Electroencephalogr Clin Neurophysiol 1991; 78: 2–11.
Kaboodvand N, Bäckman L, Nyberg L, Salami A. The retrosplenial cortex: a memory gateway between the cortical default mode network and the medial temporal lobe. Hum Brain Mapp 2018; 39: 2020–34.
Kawashima T, Okuno H, Bito H. A new era for functional labeling of neurons: activity-dependent promoters have come of age. Front Neural Circ 2014; 8: 37.
Kitamura T, Ogawa SK, Roy DS, Okuyama T, Morrissey MD, Smith LM, et al. Engrams and circuits crucial for systems consolidation of a memory. Science 2017; 356: 73–8.
Krook-Magnuson E, Armstrong C, Bui A, Lew S, Oijala M, Soltesz I. In vivo evaluation of the dentate gate theory in epilepsy. J Physiol 2015; 593: 2379–88.
Kuramoto E, Hioki H, Furuta T, Unzai T, Nakamura KC, Kaneko T. Two types of thalamocortical projections from the motor thalamic nuclei of the rat: a single neuron-tracing study using viral vectors. Cerebral Cortex 2009; 19: 2065–77.
Le Gal La Salle G. Long-lasting and sequential increase of c-fos oncoprotein expression in kainic acid-induced status epilepticus. Neurosci Lett 1988; 88: 127–30.
Lewczuk E, Joshi S, Williamson J, Penmetsa M, Shan S, Kapur J. Electroencephalography and behavior patterns during experimental status epilepticus. Epilepsia 2018; 59: 369–80.
Lothman EW, Bertram EH, Bekenstein JW, Perlin JB. Self-sustaining limbic status epilepticus induced by 'continuous' hippocampal stimulation: electrographic and behavioral characteristics. Epilepsy Res 1989; 3: 107–19.
Lothman EW, Stringer JL, Bertram EH. The dentate gyrus as a control point for seizures in the hippocampus and beyond. Epilepsy Res 1992; 7: 301–13.
McGaugh JL. Memory—a century of consolidation. Science 2000; 287: 248–51.
McGinley MJ, Westbrook GL. Hierarchical excitatory synaptic connectivity in mouse olfactory cortex. Proc Natl Acad Sci U S A 2013; 110: 16193–8.
Milczarek MM, Vann SD, Sengpiel F. Spatial memory engram in the mouse retrosplenial cortex. Curr Biol 2018; 28: 1975–80.e6.
Mohedano-Moriano A, de la Rosa-Prieto C, Saiz-Sanchez D, Ubeda-Bañon I, Pro-Sistiaga P, de Moya-Pinilla M, et al. Centrifugal telencephalic afferent connections to the main and accessory olfactory bulbs. Front Neuroanat 2012; 6: 19.
Morgan JI, Cohen DR, Hempstead JL, Curran T. Mapping patterns of c-fos expression in the central nervous system after seizure. Science 1987; 237: 192–7.
Oh SW, Harris JA, Ng L, Winslow B, Cain N, Mihalas S, et al. A mesoscale connectome of the mouse brain. Nature 2014; 508: 207.
Pathak HR, Weissinger F, Terunuma M, Carlson GC, Hsu FC, Moss SJ, et al. Disrupted dentate granule cell chloride regulation enhances synaptic excitability during development of temporal lobe epilepsy. J Neurosci 2007; 27: 14012–22.
Paxinos G, Franklin K. Paxinos and Franklin's the mouse brain in stereotaxic coordinates. . Boston: Elsevier/Academic Press; 2013.
Peng S-J, Hsin Y-L. Altered structural and functional thalamocortical networks in secondarily generalized extratemporal lobe seizures. NeuroImage 2017; 13: 55–61.
Piredda S, Gale K. A crucial epileptogenic site in the deep prepiriform cortex. Nature 1985; 317: 623.
Preston AR, Eichenbaum H. Interplay of hippocampus and prefrontal cortex in memory. Curr Biol 2013; 23: R764–73.
Racine RJ. Modification of seizure activity by electrical stimulation. II. Motor seizure. Electroencephalogr Clin Neurophysiol 1972; 32: 281–94.
Schindler K, Leung H, Lehnertz K, Elger CE. How generalised are secondarily "generalised" tonic–clonic seizures? J Neurol Neurosurg and Psych 2007; 78: 993–6.
Sheng M, Greenberg ME. The regulation and function of c-fos and other immediate early genes in the nervous system. Neuron 1990; 4: 477–85.
Stensola T, Moser EI. Grid cells and spatial maps in entorhinal cortex and hippocampus. In: Buzsaki G, Christen Y, editors. Micro-, meso- and macro-dynamics of the brain. Cham: Springer; 2016. p. 59–80.
Sugar J, Witter M, van Strien N, Cappaert N. The retrosplenial cortex: intrinsic connectivity and connections with the (para)hippocampal region in the rat. An interactive connectome. Front Neuroinform 2011; 5: 7.
Suh J, Rivest AJ, Nakashiba T, Tominaga T, Tonegawa S. Entorhinal cortex layer III input to the hippocampus is crucial for temporal association memory. Science 2011; 334: 1415–20.
Sun C, Mtchedlishvili Z, Bertram EH, Erisir A, Kapur J. Selective loss of dentate hilar interneurons contributes to reduced synaptic inhibition of granule cells in an electrical stimulation-based animal model of temporal lobe epilepsy. J Comp Neurol 2007; 500: 876–93.
Telfeian AE, Connors BW. Layer-specific pathways for the horizontal propagation of epileptiform discharges in neocortex. Epilepsia 1998; 39: 700–8.
Tonegawa S, Liu X, Ramirez S, Redondo R. Memory engram cells have come of age. Neuron 2015; 87: 918–31.
Van Landingham KE, Lothman EW. Self-sustaining limbic status epilepticus. I. Acute and chronic cerebral metabolic studies: limbic hypermetabolism and neocortical hypometabolism. Neurology 1991; 41: 1942–9.
Vertes RP, Linley SB, Groenewegen HJ, Witter MP. Thalamus. In: Paxinos G, editor. The rat nervous system. 4th edn. San Diego: Academic Press; 2015. p. 335–90.

Weiler N, Wood L, Yu J, Solla SA, Shepherd GMG. Top-down laminar organization of the excitatory network in motor cortex. Nat Neurosci 2008; 11: 360.

Wenzel M, Hamm JP, Peterka DS, Yuste R. Reliable and elastic propagation of cortical seizures *in vivo*. Cell Rep 2017; 19: 2681–93.

Westbrook GL. Seizures and epilepsy. In: Kandel E, Schwartz JH, and Jessell T, editors. Principles of neural science. 4 edn. New York: McGraw Hill; 2000. p. 910–35.

Westbrook GL. Seizures and epilepsy. In: Kandel E, Schwartz JH, and Jessell T, editors. Principles of neural science. 5th edn. New York: McGraw Hill; 2015. p. 1116–39.

White LE, Price JL. The functional anatomy of limbic status epilepticus in the rat. I. Patterns of 14C-2-deoxyglucose uptake and Fos immunocytochemistry. J Neurosci 1993; 13: 4787–809.

Yamawaki N, Corcoran KA, Guedea AL, Shepherd GMG, Radulovic J. Differential contributions of glutamatergic hippocampal/retrosplenial cortical projections to the formation and persistence of context memories. Cerebral Cortex 2018; 29: 2728–36.

Yang B, Treweek JB, Kulkarni RP, Deverman BE, Chen CK, Lubeck E, et al. Single-cell phenotyping within transparent intact tissue through whole-body clearing. Cell 2014; 158: 945–58.

York GK III, Steinberg DA. Hughlings Jackson's neurological ideas. Brain 2011; 134: 3106–13.